

25.10 A Super-Regenerative Radio on Plastic Based on Thin-Film Transistors and Antennas on Large Flexible Sheets for Distributed Communication Links

Liechao Huang, Warren Rieutort-Louis, Yingzhe Hu, Josue Sanz-Robinson, Sigurd Wagner, James C. Sturm, Naveen Verma

Princeton University, Princeton, NJ

Large-area electronics presents new form factors, enabling ubiquitous systems that are flexible and capable of scaling to very large areas. By processing thin-film transistors (TFTs) at low temperatures on plastic (using organics, amorphous silicon, metal oxides, etc.), blocks such as ADCs, amplifiers, and processors can be realized [1,2]; however, aside from short-range RFID tags [3], wireless links for long-range communication have not been achieved. A key challenge is that wireless systems typically depend on the ability to generate and operate at high frequencies, yet TFTs are limited to very low performance ($f_t \sim 1\text{MHz}$). Specifically, the challenge is low device g_m , due to low mobility and limited gate-dielectric scalability, as well as high device capacitance, due to limited feature scalability and large overlaps for alignment margining on flexible substrates. This work presents a super-regenerative (SR) transceiver with integrated antenna on plastic that leverages the attribute of large area to create high-quality passives; this enables resonant TFT circuits at high frequencies (near f_t) and allows for large antennas, maximizing the communication distance. The resulting carrier frequency is 900kHz, and the range is over 12m (at 2kb/s). As shown in Fig. 25.10.1, this will enable sheets with integrated arrays of radio frontends for distributing a large number of communication links over large areas.

Figure 25.10.1 shows the transceiver architecture. The circuits are based on amorphous-silicon (a-Si) TFTs processed at 180°C [4]. The critical block is an LC oscillator. The tank inductors act as the antenna. In TX mode, data is transmitted by gating the oscillator for on-off-keying (OOK) modulation; in RX mode OOK data is received by sensing the oscillator startup time with respect to a quench signal. The design is based on three key insights: (1) LC oscillators offer the benefit that performance limitations due to TFTs can be overcome by the ability to form high-quality passives (as described in the next paragraph); (2) the ability to pattern large inductor antennas, with dimensions on the order of a meter, substantially improves coupling between transmit and receive antennas; and (3) active transceivers result in superior scalability in communication distance as compared to a passive transponder. Figure 25.10.2 illustrates how these factors enhance communication distance. At the achieved frequency, the carrier wavelength is $\sim 300\text{m}$, implying that the antennas are electrically small and, for the distances of interest, operate dominantly in near-field mode. In this case, antenna coupling is determined by mutual inductance (M), which greatly improves with large antennas, as shown. In the near field, inductor coupling also makes communication based on impedance modulation possible, enabling a passive transponder. However, Fig. 25.10.2 shows that the received signal due to a reflected impedance degrades quadratically with M , thus falling rapidly with distance; whereas the received signal due to an active transmitter degrades only linearly with M , enabling the distance achieved in this work.

Figure 25.10.3 shows details of the LC oscillator, including the gate resistance, R_g ($\sim 50\Omega$ for a bottom-gate TFT structure) and load capacitance of the subsequent block, C_L (i.e., envelope detector). The positive-feedback oscillation condition requires that $g_m R_{\text{tank}} > 1$ for the cross-coupled stages. As shown, this condition can be written as a term that depends on the performance of the TFTs g_m / C_{tank} and a term that depends primarily on the quality of the inductors $L / (R_{\text{ind}} + R_g)$; the second term benefits from inductor area scaling, enabling robust oscillations, as described in [5]. The voltage induced in a receive antenna due to the current in a transmit antenna i_{ind} is given by $M(di_{\text{ind}}/dt)$. With M depending on physical parameters of the antennas and their distance, the power efficiency of the transmit oscillator can thus be represented by normalizing di_{ind}/dt with the current consumed by the oscillator $i_{\text{osc}}: (1/i_{\text{osc}})di_{\text{ind}}/dt$. Figure 25.10.3 shows that this quantity is maximized by minimizing C_{tank} (i.e., $C_{\text{TFT}} + C_L + C_{\text{ind}}$) and $R_{\text{ind}} + R_g$. Inductor area scaling helps with both of these. First, patterning thick planar traces leads to low R_{ind} , leaving R_g . Second, C_{ind} benefits from patterning inductor traces with adequate separation, leaving C_{tank} limited by the TFT and load capacitances. The TFT parasitics are roughly $C_{gs/d} \sim 7\text{pF}$,

$C_{ox} \sim 5\text{pF}$, $R_g \sim 50\Omega$, and for the coupled $0.6\text{m} \times 1.2\text{m}$ inductors used, $L_{\text{ind}} \sim 180\mu\text{H}$, $R_{\text{ind}} \sim 4\Omega$, $C_{\text{ind}} \sim 10\text{pF}$. To drive C_L ($\sim 20\text{pF}$) at an oscillator voltage (V_{swing}) of 10V with the circuit values used, i_{osc} is measured to be $500\mu\text{A}$ from a 20V supply.

Figure 25.10.4 shows the envelope detector and comparator. The oscillator signal is AC coupled to the envelope detector. The primary concern is ensuring that high-frequency components do not conduct to the output via the TFT gate-source capacitances. In the topology, rectification is achieved by the non-linear TFT currents on the source node, and the capacitive transmission effect is cancelled by the differential structure, where $C_{gs1,2}$ pull the source node in opposite directions.

The availability of only NMOS TFTs in the standard a-Si technology poses challenges for achieving strong regeneration in the comparator. In the topology used, the NMOS regenerative devices are in the pull-down path, in series with the input devices. Although a parallel regenerative path would lead to faster regeneration, the input devices in series improve sensitivity and robustness by making the regeneration path explicitly dependent on the input signal. This also mitigates matching issue since the matching now dominantly relies on the input pair. To further enhance robustness, the TFT lengths are upsized to $10\mu\text{m}$, rather than $6\mu\text{m}$, which is used for all other devices in the radio and is roughly the limit for high yield in our TFT process on plastic. To ensure sufficient strength of the regenerative path, the biasing point of the input devices, set by the envelope detector output, is maximized. For this, the envelope detector inputs and tail current are biased, so that the output is at the highest level at which the RX-mode oscillator swing (5V) can be tracked without being saturated by V_{DD} . Biasing is achieved using thin-film doped a-Si resistive dividers.

Figure 25.10.5 shows the control block. A baseband processor, which can be placed at a distant location on the sheet, provides clock, data, and TX/RX-selection signals via patterned large-area interconnects. The capacitance between two large-area interconnects separated by 1cm is roughly 44fF/m. To enable synchronization of the radio, clock (CLK) is used to derive the oscillator tail-control (TAIL) and comparator-enable (CMPR) signals, as shown. In RX mode, TAIL is a quench signal (QUENCH); when CLK is high, QUENCH is set by the voltage divider to a low value that suppresses oscillations. Then, to maximize receiver sensitivity, a gradual turn-on is desired [6]; this is achieved by using a weak NMOS device (M_1) to charge QUENCH. CMPR is then derived from a delay chain, to position the comparator decision instance at a point just before that where the oscillator would start up in the absence of receive data. In TX mode, TAIL is a full-swing signal derived from the transmit data, and it is used to switch the oscillator for OOK modulation.

Figure 25.10.6 shows measured waveforms from the prototype fabricated on $50\mu\text{m}$ polyimide, which is shown in Fig. 25.10.7. For data rates of 2kb/s and 4kb/s the communication distances are 12m and 7m (BER < 0.1%) respectively, achieved using the $0.6\text{m} \times 1.2\text{m}$ antennas, and with measured receiver sensitivity of -80dBm . With a 20V supply, the total RX/TX power consumption is $2.2\text{mW}/5\text{mW}$.

Acknowledgements:

We thank NSF for funding through grants ECCS-1202168 and CCF-1218206.

References:

- [1] K. Myny, et al., "An 8b Organic Microprocessor on Plastic Foil", *ISSCC Dig. Tech. Papers*, pp. 322 - 324, Feb. 2011.
- [2] W. Xiong, et al., "A 3V 6b Successive-Approximation ADC Using Complementary Organic Thin-Film Transistors on Glass", *ISSCC Dig. Tech. Papers*, pp. 134-135, Feb. 2010.
- [3] K. Myny, et al., "Bidirectional Communication in an HF Hybrid Organic/Solution-Processed Metal-Oxide RFID Tag", *ISSCC Dig. Tech. Papers*, pp. 312-313, Feb. 2012.
- [4] B. Hekmatshoar, et al., "Highly Stable Amorphous-silicon Thin-film Transistors on Clear Plastic," *Appl. Phys. Lett.*, vol. 93, no. 3, July 2008.
- [5] Y. Hu, et al., "Flexible Solar-Energy Harvesting System on Plastic with Thin-film LC Oscillators Operating Above ft for Inductively-coupled Power Delivery", in *IEEE Custom Integrated Circuits Conf.*, pp. 1-4, Sept. 2012.
- [6] J. L. Bohorquez, et al., "A 350 μW CMOS MSK Transmitter and 400 μW OOK Super-Regenerative Receiver for Medical Implant Communications", *IEEE J. Solid-State Circuits*, vol. 44, Issue: 4, pp. 1248-1259, Apr. 2009.

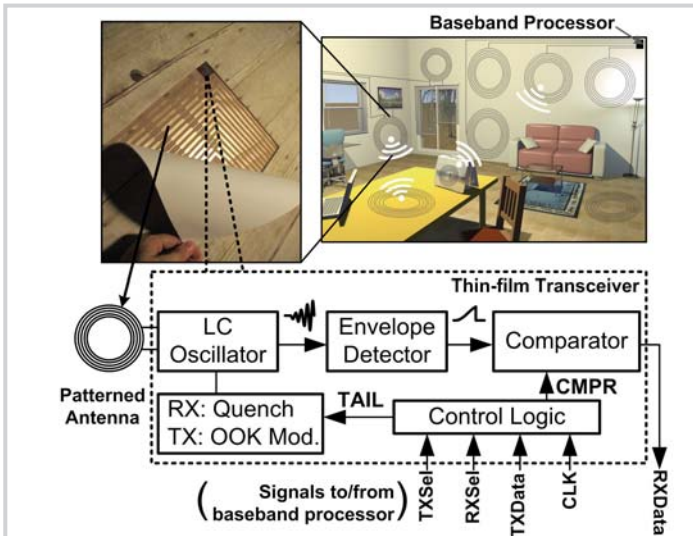


Figure 25.10.1: Architecture of the super-regenerative transceiver fabricated on large-area plastic sheets.

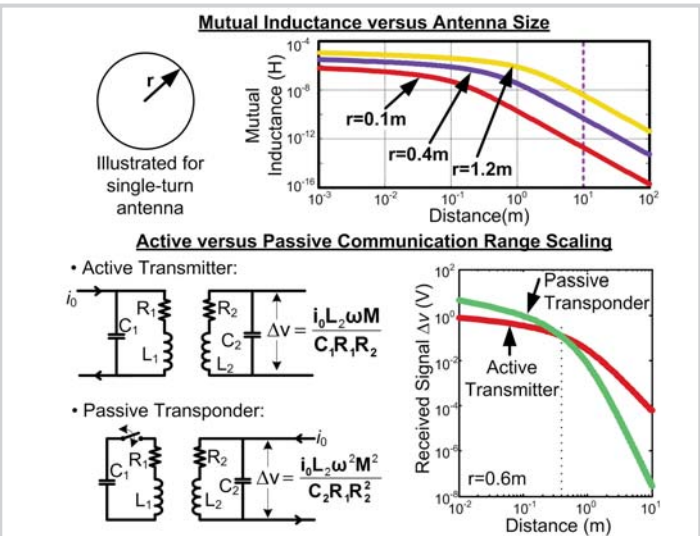


Figure 25.10.2: Analysis for communication distance; large antennas increase M, and active transmitters yield superior distance scaling.

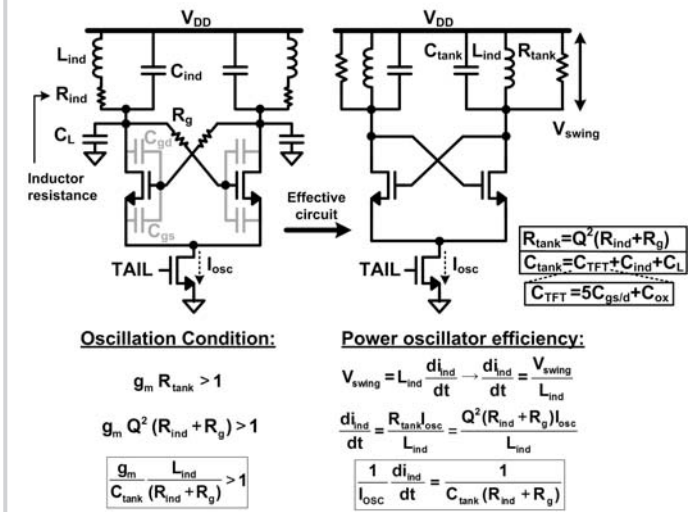


Figure 25.10.3: Analysis of thin-film LC oscillator for transmitter front-end (tail quench signal used for OOK modulation).

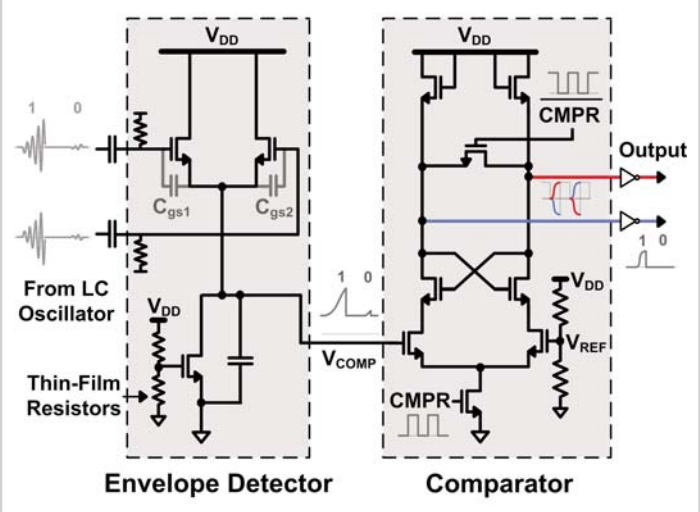


Figure 25.10.4: Thin-film envelope detector and comparator; differential envelope detector enables rectification of high frequencies.

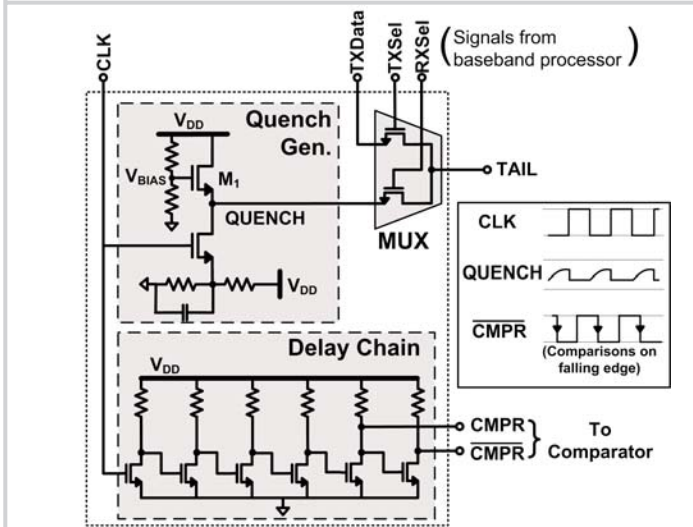


Figure 25.10.5: Thin-film control block for oscillator quench and comparator-enable signals in RX mode and OOK in TX mode.

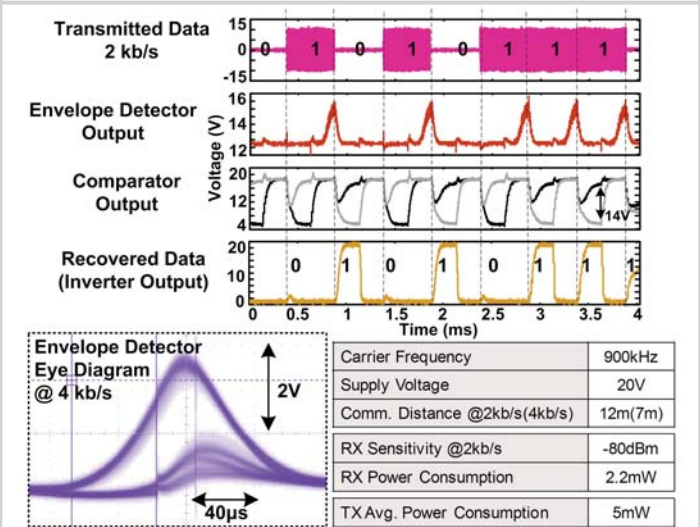


Figure 25.10.6: Measured waveforms and performance summary of the thin-film radio on plastic.

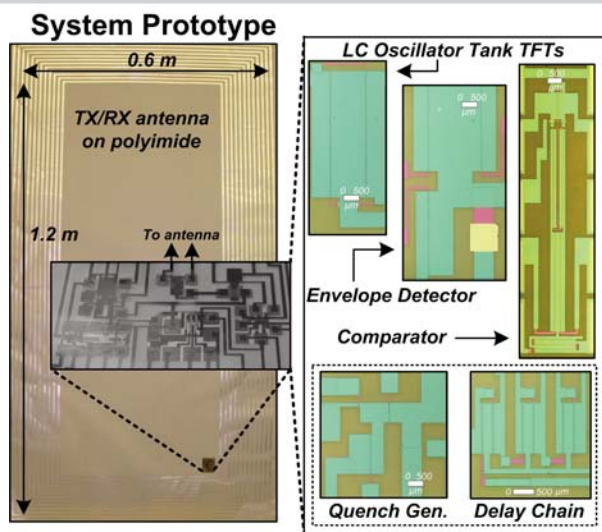


Figure 25.10.7: Prototype on plastic, including large antenna patterned on polyimide; all of the thin-film circuits are fabricated in-house on 50 μm -thick polyimide foil.